A BENCHMARK STUDY ON PRINTING PDMS ON A HYDROGEL FILM IN BOTTOM-UP VAT PHOTOPOLYMERIZATION

A Thesis

by:

FEIMO YANG

Submitted to the Graduate and Professional School of
Texas A&M University
in partial fulfillment of the requirements for the degree of

MASTER OF SCIENCE

Chair of Committee,	Bruce Tai
Committee Members,	Matt Pharr
	Melissa Grunlan
Head of Department,	Guillermo Aguilar

May 2022

Major Subject: Mechanical Engineering

ABSTRACT

The separation between printed part and vat floor in constrained surface vat photopolymerization (VP) is a crucial issue, which limits the printability on different materials and the overall printing speed. This study aims to characterize the separation behavior of a photo-curable PDMS resin with hydrogel vat film in comparison to a convention baseline of commercial acrylate-based resin with PTFE film. A DLP printer is modified with an in-situ force measuring capability. 8 test cases with unique combinations of three factors (film, resin, and separation speed) are developed. The results found that all three factors influence the separation. A faster speed leads to a higher separation force but generally shorter separation distance. Hydrogel film demonstrates lower separation force and shorter separation distance than PTFE film. Photocurable PDMS resin shows lower separation force but longer separation distance than commercial acrylate-based resin. Moreover, the analyzed results also indicate all factors are significant, and have a general trend regardless of other factors.

ACKNOWLEDGEMENTS

I would like to thank my committee chair, Dr. Bruce Tai for his continuous motivation, guidance, and support throughout the research.

Moreover, I would like to thank my committee members Dr. Matt Pharr and Dr. Melissa Grunlan for serving on my advisory committee.

Furthermore, I would like to acknowledge the support from XYZ Printing for providing the DLP printer, the printing materials, and the vat films for this project. I would also like to appreciate Nick Kang, Kevin Chen, and Yuchen Chang for their technical supports.

I would also like to thank Dr. Melissa Grunlan and Alec Marmo for their support on the printing materials and valuable inputs.

Finally, I would like to thank all my lab mates for their valuable inputs throughout the research.

CONTRIBUTORS AND FUNDING SOURCES

Contributors

This work was supervised by a thesis committee consisting of Dr. Bruce Tai (Advisor), Dr. Matt Pharr and Dr. Melissa Grunlan of the Department of Biomedical Engineering.

The preliminary design of the experiment setup was done by Aamer Kazi from Texas A&M University.

All other work related to the thesis was conducted by the student independently.

Funding Sources

Graduate study was supported by a fellowship from Texas A&M University.

TABLE OF CONTENTS

LIST OF TABLES

Page

LIST OF FIGURES

Page

1. INTRODUCTION

1.1 Background and Literature Review

Vat photopolymerization (VP) is an additive manufacturing (AM) technology in which exhibit superior resolution and accuracy, while maintaining decent surface quality [1]. The technology was first introduced in the 1980s on a patent on stereolithography (SLA) [1,2,3], and has evolved in the past decades with innovative approaches to selectively convert a photocurable liquid into a solid under ultraviolet (UV) light exposure [2,3]. This light source can be applied in two distinct orientations: free surface approaches or constrained surface approaches. [4,5] In the free surface VP, the building platform, where prints build on, is placed in a tank of resin. The UV light directly illuminates on the designed cross-section which cures the layer. Each subsequent layer builds on the previous layers as the platform further lowers into the tank [6]. The constrained surface VP, or bottom-up VP, utilized the suspended building platform above a resin tank. The UV light illuminates from below, through the transparent tank floor and cures the resin. The resin is constrained between the building platform or printed part and vat floor. Every new layer is built as the platform elevates. Unlike the free surface approach, a constrained surface needs a minimum amount of resin because the printed part does not need to be fully submerged in the resin [6]. However, a crucial limiting factor of constrained surfaces is the separation process required to overcome the attractive interaction between printed part and vat floor for each new layer [6,7]. This undesired interaction limits printing cross-sectional area, printing speed and causes printing failure if it sticks to the vat floor [8,9].

Many attempts to reduce this undesired interaction. The conventional approach to address this interaction is applying a low surface energy film material on top of the vat floor.

Polytetrafluoroethylene (PTFE) is the most common material used for this purpose, due to their known low surface energy. However, the reduced interaction is still insufficient for fragile printing materials and prints [6]. Another available approach is applying an oxygen permeable film which creates a thin oxygen layer on top of the vat floor. This oxygen layer works as a curing inhibitor to prevent contact interactions between prints and vat floor, thus eliminating this unwanted interaction. Nevertheless, maintaining the oxygen layer's concentration and uniformity is technically challenging and varies between materials and environments [8]. Another attempt aimed to use a vibration-assisted system on the build platform to facilitate separation between prints and vat floor. The results showed a promising reduction in separation forces, yet with vibrations, small features and fragile materials could be damaged [10]. Due to such limitations in chemical and physical approaches, the contact base film, like PTFE, is still preferred because of its simplicity and no hardware modification required. In a more recent development, an innovative hydrogel film, namely Ultra-Fast Fabrication (UFF) technology (XYZ Inc. Taiwan), is introduced to replace the conventional vat film. The high-water content (up to 90%) in the film creates a natural repelling force to non-polar photopolymers, and thus reduces the interaction between non-polar prints and polar vat floor. This technology can speed up the vat photopolymerization process and potentially enable printing of fragile or soft materials, such as polydimethylsiloxane (PDMS), which is a widely used silicone rubber [12]. However, the study on this film is still limited.

PDMS printing has drawn lots of attention recently because of its applications in various fields like electronic, robotics, and biomedical devices, as it exhibits high optical transparency, biocompatibility, and flexibility [11,12]. Many studies are limited to the extrusion-based printing method, such as direct ink writing (DIW), because of the liquid form that PDMS precursor is in [12,13,14]. However, due to its low viscosity and low elastic modulus, extrusion-based printing

might not be the best approach [13,15]. A prior study by the authors has shown the printability of a photocurable PDMS via VP [11]. Due to PDMS' low modulus and strength (the pure PDMS without any fillers), its printing was limited by separation issue, which greatly increased the total manufacturing time [8]. Another disadvantage of this PDMS resin is its brittleness that leads to potential layer separation and distortion during high-speed printing [8]. Therefore, it is of interest to see if the hydrogel can improve the printability of PDMS in vat photopolymerization. For this, the objective of this study is to conduct a full factorial study using hydrogel and PTFE as two interfacial films, and PDMS and regular acrylate-based resin as two printing materials, where PTFE film and acrylate are the baseline materials. The experiment is to compare the separation behavior quantitatively in terms of the overall force profile, magnitude of separation force, and separation distance. Moreover, because of the brittle characteristic presented in PDMS, it is necessary to consider the influence of separation speed for a more comprehensive understanding. In this work, a modified constrained surface digital light processing (DLP) printer is used to capture the in-situ separation force through an entire printing which contains multiple separation events.

Many have attempted to measure the in-situ separation force including mounted load cell on the building platform and modification of the vat with force sensors [6,8,10]. Some studies focused only on the maximum pulling force when comparing the separation force reduction without looking into the force profile over the distance/time, others only measured profile for one given film and resin, which did not provide more insight on separation process between materials. Therefore, a combination of both will provide more understanding of the separation. For example, separation distance (where the force drops to zero) is crucial for optimizing the motion of building platform during the printing process, which can eliminate unnecessary ascending distance, thus

shortening the overall printing time; However, this may vary from film to film and resin to resin. In this study, the in-situ force data is achieved by an embedded piezo-electric sensor in the build platform sampled over 1 kHz, allowing more comprehensive data for the benchmark study.

1.2 Research Objectives and hypotheses

The objective of this research is to analyze the separation behaviors of a photocurable PDMS resin with hydrogel film, in comparison to a benchmark case, a commercial acrylic resin with PTFE film. These behaviors are in terms of the overall force profile, force magnitude, and separation distance. A constrained surface Digital Light Processing (DLP) system is used and modified for this purpose, aimed to measure the in-situ forces during the entire printing process that has multiple separation events. With continuous exampling of the force data, the trend of each resin and film combination should be captured, and their maximum separation forces and separation distances can be also determined. The hypotheses, as mentioned in previous section, are that hydrogel film will reduce the separation force in both PDMS resin and acrylate-based resin. It is because their non-polar and hydrophobic properties. However, it is unknow how the distance may change, but it may be related to the material properties of both resins and films. As the separation will introduce pressure on the separating surfaces, how they would deform may also need to be considered here.

2. METHODOLOGIES AND PROCEDURES

2.1 Experimental Setup and Printing Parameter

FIGURE 1a shows the commercial XYZ Nobel Superfine DLP printer used (XYZ printing, New Taipei, Taiwan). The building platform can hold a maximum build size of 64 mm × 40 mm × 120 mm, with an XY- resolution of 50 µm and Z-resolution of 25 µm. The printing parameters for commercial acrylate-based resin (Superfine UV Resin Clear) were given by the manufacturer, shown in Table 1. The resin was a clear liquid at room temperature and contained 25-35% Urethane Acrylate, 50-60% Acrylic Monomer, 5-10% Trimethylolpropane Triacrylate, and 0-5% Photoinitiator [16]. The photocurable PDMS resin was synthesized in house and contained liquid methacrylate PDMS-macronmer and a 2Wt.% commercial photoinitiator, TPO-L (Combi-Blocks Inc., San Diego, CA). The detailed synthesizing procedures, chemical structures, and printing parameters for photocurable PDMS follows the previous work published elsewhere [11,17]. The printing parameters for this resin shown in Table 2. The photocurable PDMS resin was also transparent at room temperature.

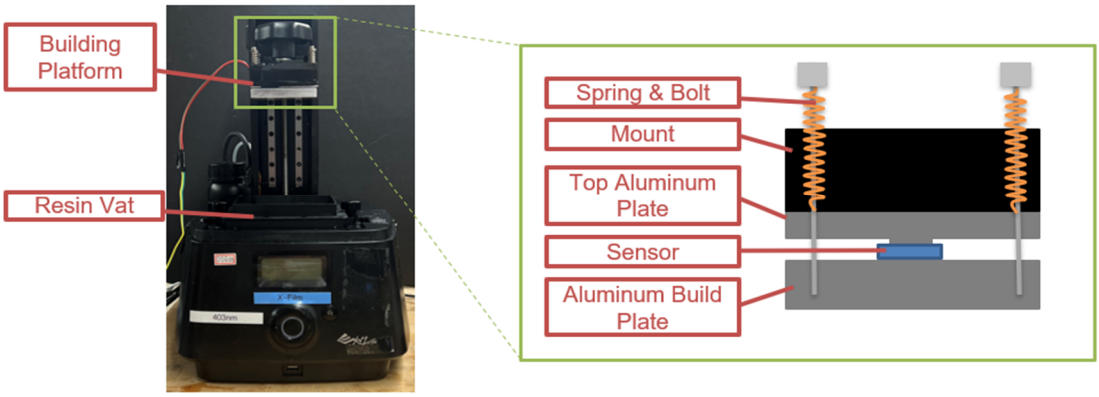

(a) (b)

FIGURE 1: A bottom-up DLP printer with in-situ force measuring. (a) DLP printer (b) modified building platform

The building platform was modified and mounted with a thin-film compression sensor, FlexiForce™ A101 Sensor (Tekscan Inc., Massachusetts), to measure the separation force continuously. The modified building platform consisted of five components, as summarized in Figure 1b. The mount, which connected the platform to the printer, as well as two aluminum plates, which clipped the sensor in between and the top one rigidly attached to the mount. In addition, the springs and screws connected the whole assembly, which provided a compressive force to the sensor and preloaded the sensor. Because of this preload applied, the sensor could measure both tensile and compressive forces during the printing.

TABLE 1. Printing parameters used for acrylate-based resin

Printing parameters	Set values
Exposure time	1.4s
Power density	70W/m^2
Separation distance	3mm
Wait time	0.5s

TABLE 2. Printing parameters used for photocurable PDMS resin

Printing parameters	Set values
Exposure time	10s
Power density	100W/m^2
Separation distance	3mm
Wait time	0.5s

The compression sensor had a 0.203 mm thickness which could be fit in the building platform design and a 5 μs fast response time which suited our purpose on in-situ monitoring. The circuit used for the force sensor can be found in the datasheet elsewhere from manufacturer [18]. This compression sensor was a force-sensitive resistor, which changes its resistance upon

compressive force applied. The NI DAQ PCIe-6321 (NI inc., Texas) used for data collection, also acting as a vision aid on in-situ force measured. The setup collected the force data at a 1,000 Hz sampling rate. Before the experiment, the sensor was calibrated to precisely convert the digital voltage readings to forces, and calibration setup is shown in FIGURE 2a. The setup was preloaded at maximum voltage range, this is accomplished by moving the horizontal slide towards the building platform. This compressive force is measured and showed in real-time, as the compressive force reaches the maximum reading on the sensor, which is around 5V, we added pulling force to the center of the building platform while measuring it through a digital force gauge with a resolution of 0.1N, OMEGA DFG35- 20 (Omega Engineering Inc., Connecticut). With a 10k ohms feedback resistor in the sensor circuit, the calibration curve is obtained as shown in FIGURE 2b where the linear region of force measurement was between 20N to 55N. Therefore, a preload around 45N was used for this experiment.

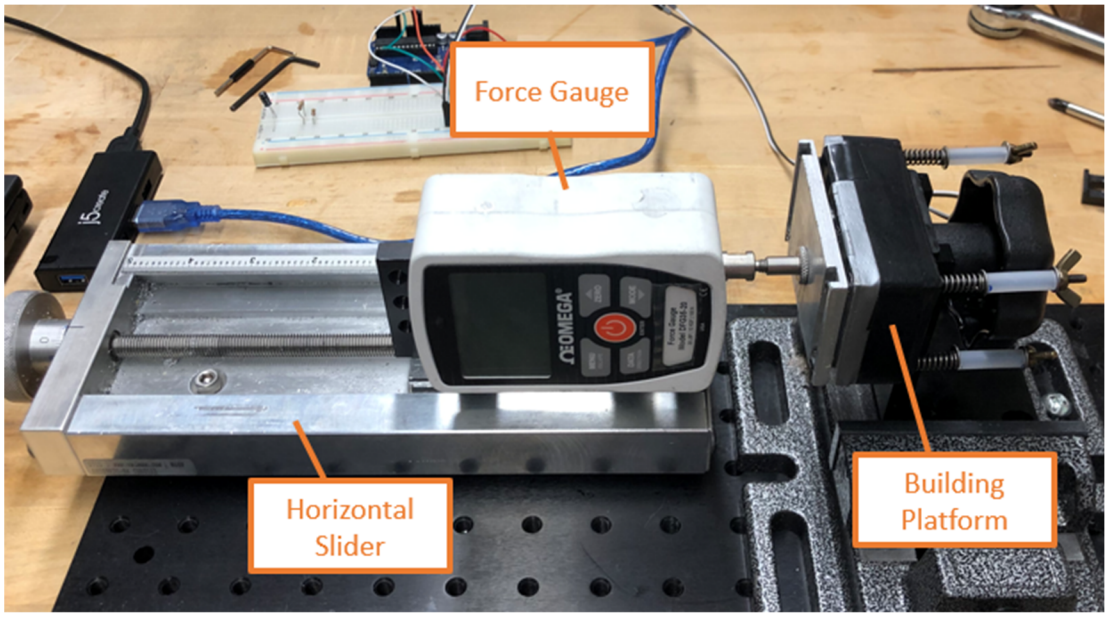

(a)

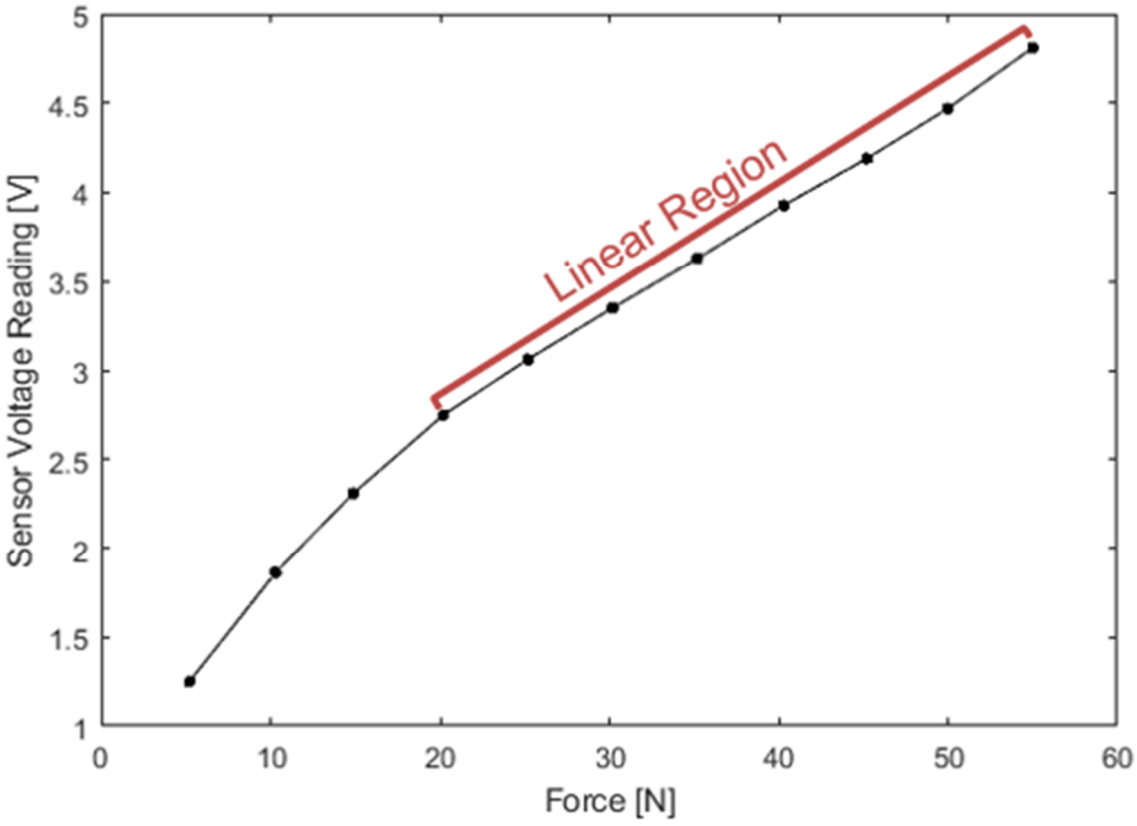

(b)

FIGURE 2: Sensor calibration (a) setup and (b) curve

2.2 Film Preparation

The PTFE film was commercially available from the manufacturer for the DLP printer used and it was tailored to fit the vat floor. The hydrogel film was synthesized following the procedure provided by the manufacturer, which consisted of non-polyelectrolyte and water colloid, as well as polyelectrolyte, and coagulant. The synthesis details can be found in the patent application [19]. The hydrogel film was trimmed to fit into the vat. FIGURE 3 shows these two films. The PTFE film was translucent and visually flat sheet with minimal light distortion. The hydrogel film was nearly transparent yet appeared to have some light distortion due to its surface texture. However, it was unknown how these visual differences may affect the separation process. PTFE film had a thickness of 0.2mm, and its uniform throughout the exposed surface in the vat. Hydrogel film had an average thickness of 2.5 mm, which varied slightly (~0.1mm) due to in house manufacturing.

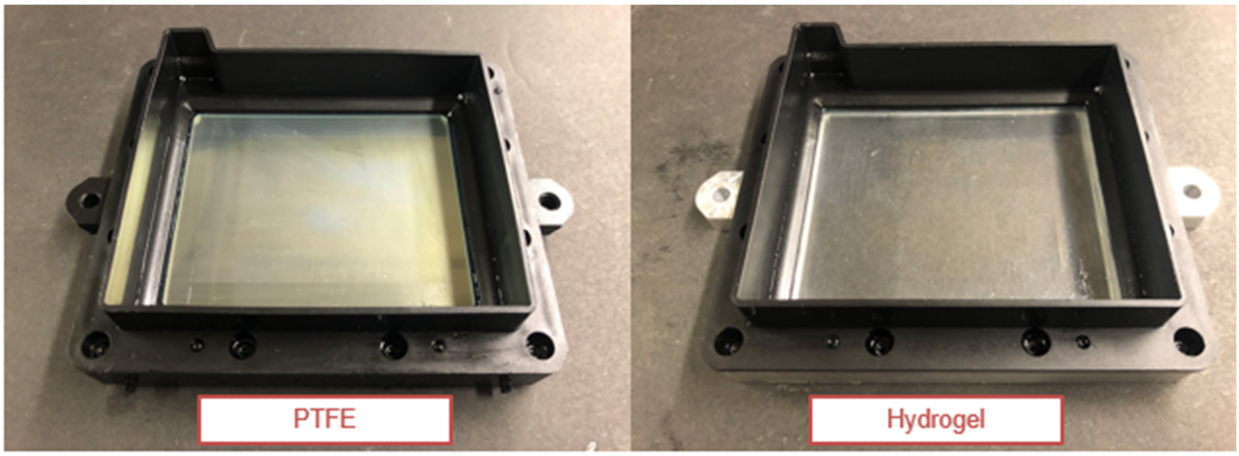

FIGURE 3: PTFE film in vat and hydrogel film in vat

The UV light transmittance was also measured with the printer's light source, and the values are 94% and 99% for PTFE and hydrogel, respectively. This transmittance is measured

using a EO laser power & energy meter (gentec-eo, Ontario, Canada). The light intensity of the UV light source on the DLP printer is measured directly without any film, and then compared with the intensity of those with the two different films.

2.3 Design of Experiment and Data Reduction

This experiment measured the separation of a 25 mm × 25 mm cross-sectional area for 50 layers. The cross-sectional area was tested prior to the experiment. This is to ensure a sufficient separation force will occur through the experiment, and also to avoid the excessive force beyond the measurement range. The number of layers is chosen to ensure the position of the building platform, while the separation happens, is always submerged in the resin slurry. The layer thickness is set to 50 μm. The printing parameters were identical for the same printing material for the two films (Table 1 & Table 2). To avoid any material degradation over the course of study, film and resin were replaced after every test. The sensor was preloaded to 45N prior to the start of the experiment, which provided a proper measurement range as discussed in Section 2.2. The standard DLP printing process has several base layers that need to be exposed for a longer period than the subsequent layers to build a foundation, which forms a strong adhesion between building platform and printed part [6]. For both resins, 12 base layers were built, and therefore, only force data after the base layer was used for analysis. Prior to the experiment, multiple parametric tests were conducted to acquire separation speeds suitable for all films and resins. Due to material and hardware limitations, two separation speeds (0.25 mm/s & 0.1875 mm/s) were chosen to avoid printing failures and to have a reasonable signal-to-noise ratio. A total of 8 cases with unique combinations were conducted and combinations are shown in Table 3. Each case had 34 distinct separation cycles, excluding the base layers.

TABLE 3: Design of Experiment

Case	Film	Resin	Separation Speed
1	PTFE	Acrylate-based	0.25 mm/s
2	Hydrogel		
3	PTFE	PDMS	
4	Hydrogel		
5	PTFE	Acrylate-based	0.1875 mm/s
6	Hydrogel		
7	PTFE	PDMS	
8	Hydrogel		

Through the entire 34 separation processes, the preload slightly drifts over time. FIGURE 3a shows an example of force data collected through the entire 34 layers process, which, at selected layers region, we can clearly observe a drift in preload. Therefore, dynamically defined a reference zero force for each separation cycle is needed, which identifies the start and the end for a separation. FIGURE 4b shows a single separation cycle, which is divided into four stages. First stage is an idling stage where the building platform rests above the vat film. In this stage, the motor is inactive, thus no force present here. Therefore, this stage is also considered as the reference zero for the particle separation cycle. Second start is descending, where the motor starts moving and brings the platform towards the film until the gap between platforms is enough for a new layer to cure. A compressive force occurs at the end of this stage, which is due to contact between platform and resin surface. This force continuously increases as the platform submerged into the resin, and eventually drops after it reaches the desired position. The drop is likely caused by displacement of the resin between platform and film. Third stage is the curing stage where UV projection turns on and a new layer cures under the exposure. In this stage, the motor is also inactive, yet small compressive force still occurs though this stage due to material curing. The last stage is the separation where the platform starts to ascend at a set speed and separation starts between the new

layer and film. This difference between the tensile force profile and the reference zero is defined as the separation behavior.

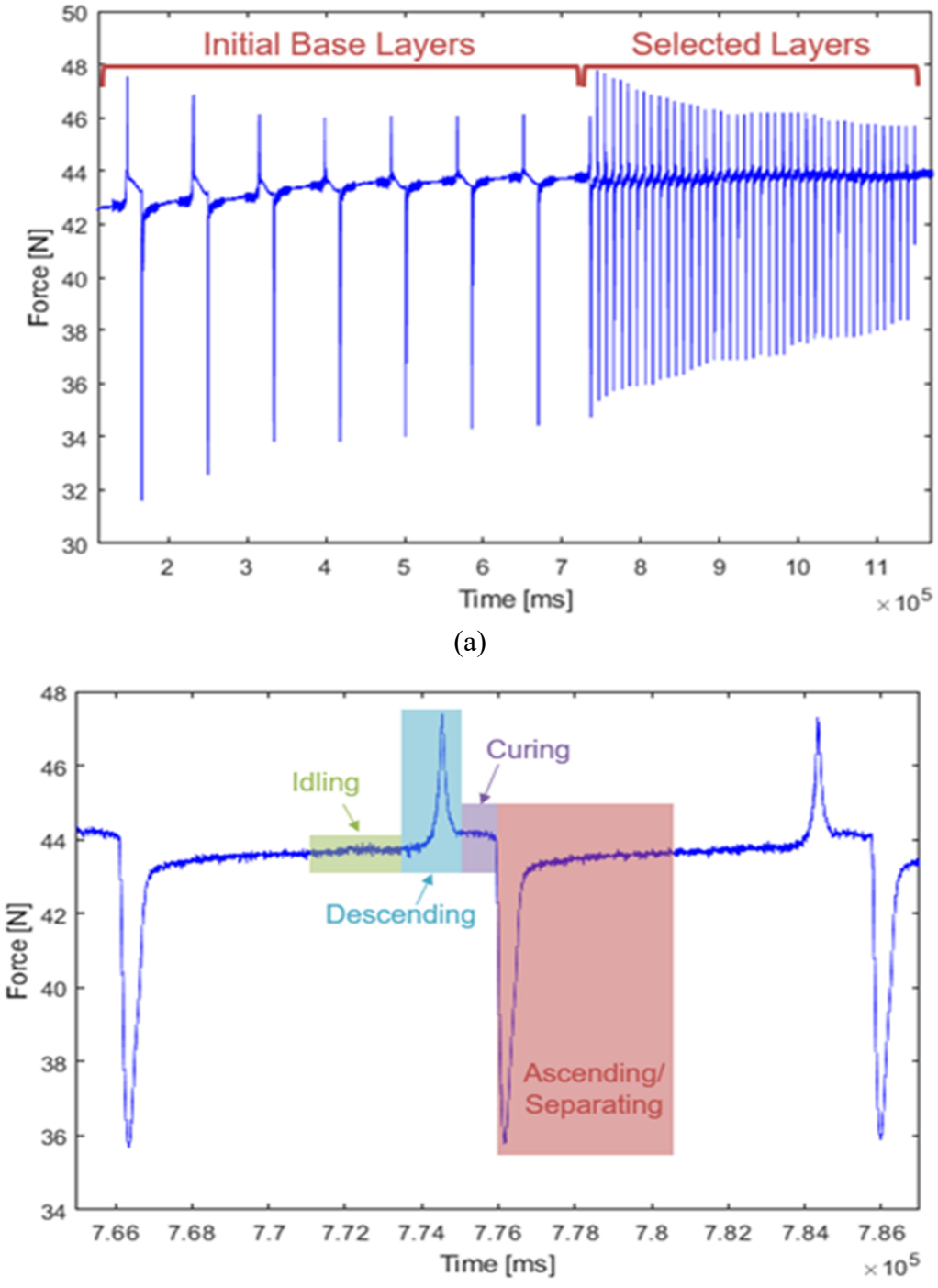

FIGURE 4: A signal example of a) a full 50 layers print; b) a single layer

3. RESULTS

3.1 Pulling Force Profiles and Observations

FIGURE 5 and FIGURE 6 show the separation profile for all eight combinations in terms of separation force and distance. FIGURE 5 groups all data of the high-speed setup (0.25 mm/s), while FIGURE 6 shows those of the low-speed setup (0.1875 mm/s). The separation forces are plotted as positive values to present as a tensile load. The x-axis is the separation distance obtained based on the constant building platform ascending speed, which is also the separation speed. The color bar on the right of each plot indicates the chronological order of each separation cycle through a 34 layers printing process. The earliest cycles are represented in blue and this color transits through green, yellow, orange and eventually red as the order of cycle increases. Furthermore, this starting point ($x = 0$) was defined when the ascending/separating region (from FIGURE 3) first crosses the value of the reference zero, which is mentioned in section 2.2.

In all eight cases, force profiles show continuous change as the cycle (the color) increases though the changes are within a small range. For the acrylate-based resin with PTFE film, the force profile starts at a higher maximum force and gradually decreases through the entire 34 layers. With the same resin but hydrogel film, a similar trend is also exhibited. Whereas, both PDMS resin cases show contrasting change, which maximum force increases through the process, instead of decreases.

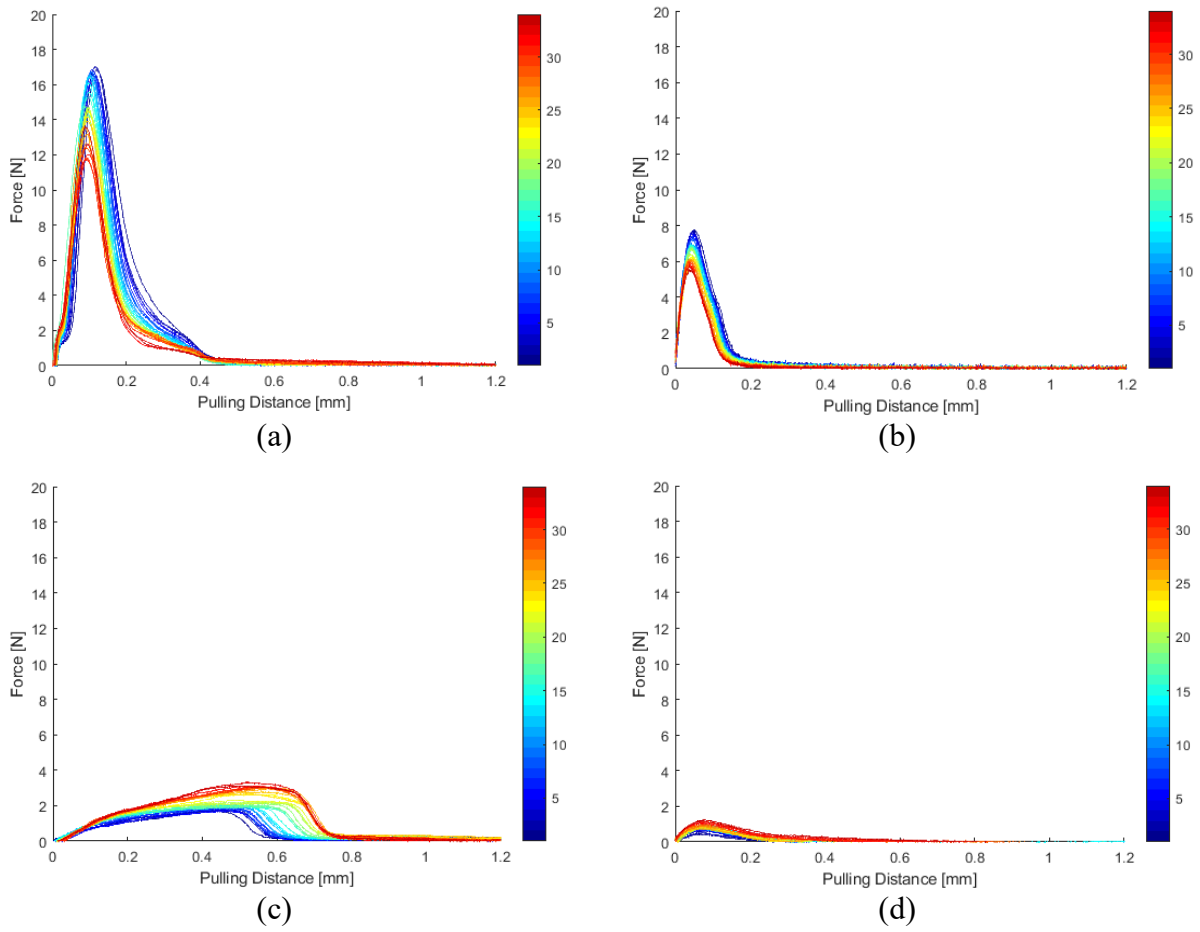

FIGURE 5: Separation forces in the process of printing a 2.5 mm tall square extrusion at 0.25mm/s ascending speed (a) Acrylate-based resin + PTFE film; (b) Acrylate-based resin + hydrogel film; (c) PDMS resin + PTFE film; (d) PDMS resin + hydrogel film;

In terms of separation distance, the benchmark case shows a more consistent value over the multiple passes, but PDMS resin with PTFE film exhibits an increase in distance as printing progressed. Furthermore, the two ascending speeds have minimal impact on the direction of this shift, where both speeds show the same trend for the same combination. At high-speed, these shifts in PTFE film exhibit a greater and more rapid transition than these in hydrogel film. However, it is less discernible at low-speed, where the forces have smaller magnitude than higher speed.

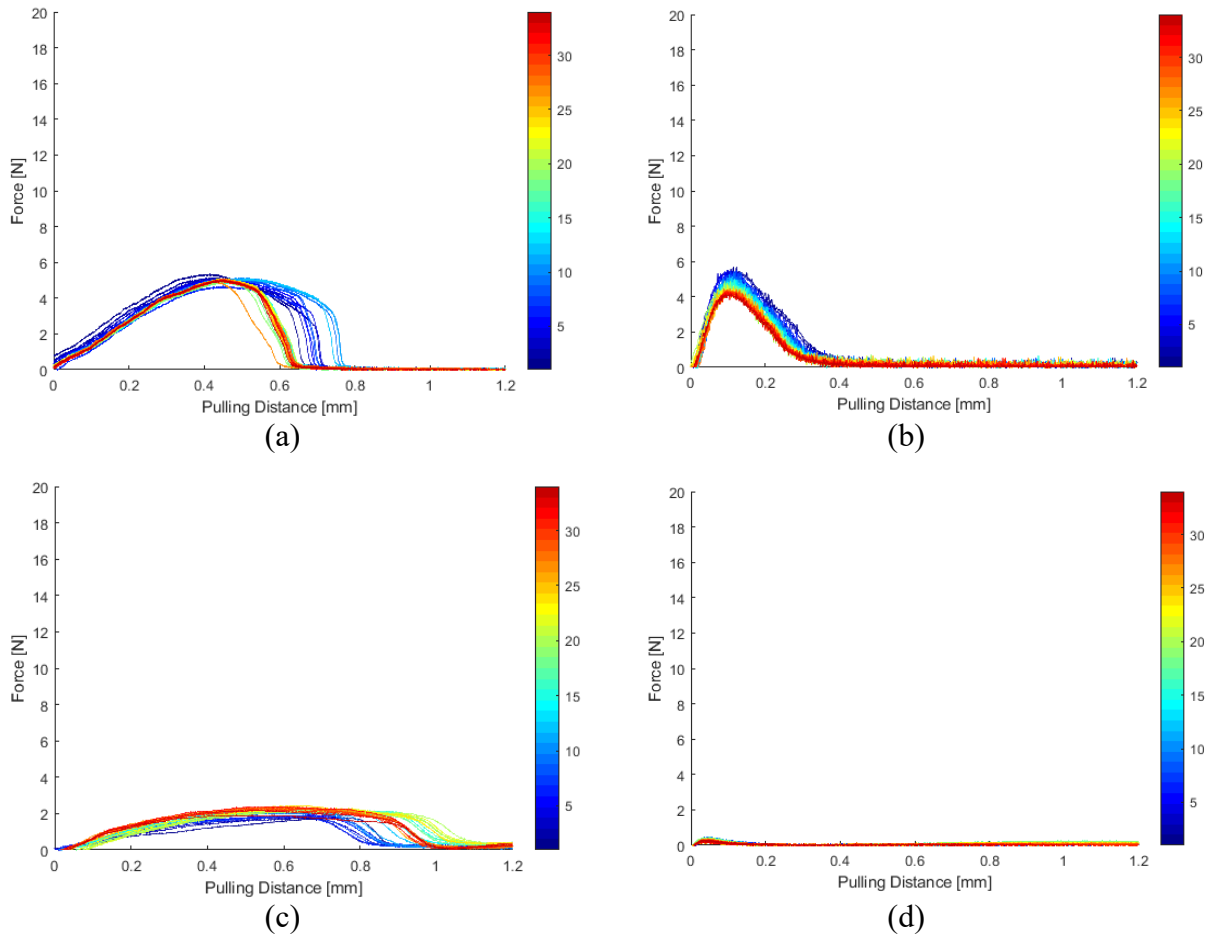

FIGURE 6: Separation forces in the process of printing a 2.5 mm tall square extrusion at 0.1875mm/s ascending speed (a) Acrylate-based resin + PTFE film; (b) Acrylate-based resin + hydrogel film; (c) PDMS resin + PTFE film; (d) PDMS resin + hydrogel film;

Replicated tests were performed on cases 1, 2, 3, 4, 5 and 8 of these eight cases and the similar trend were observed. The replicated tests results can be found in APPENDIX A. These changes reflect the material and film characteristics and combined effects. Overall, the PTFE film exhibits larger forces and longer separation distances than the hydrogel film and PDMS resin exhibits lower forces and longer separation distances than acrylate-based resin, except one case: hydrogel film at low-speed. This may be caused by extremely small separation forces in the PDMS resin with hydrogel film, which is nearly zero.

By further looking into the shapes of force profiles at high ascending speed, the benchmark case exhibits a sharp escalation in force at the start of separation, and then follows a rapid force drop after reaching the peak value. At the end of separation, this rapid decrease transits to a more moderate one. The PDMS resin with PTFE film, on the contrary, shows a gradual climb in force and then transit to a more rapid decrease without any transition at the end of separation. As for acrylate-based resin with hydrogel film case, it shows a rapid increase in the force and followed by a rapid decrease till the end of the separation. Similarly, the PDMS resin with hydrogel film shows a smooth increase, then smooth decrease without any outlying transition. At low ascending speed, the benchmark case exhibits a very different profile, which instead of a sharp increase at the front, the increase is now more moderate. Once it reaches its peak, the force slowly decreases and then follows a sharp drop near the end of complete separation. The other three cases at low speed show a relatively similar force profile to the high-speed ones. Yet, low-speed cases overall exhibit lower separation force than high-speed ones.

3.2 Statistical Analysis

To systematically compare the performance of these cases, a 3-way ANOVA was performed on the effects of separation speed, film, and resin on the two dependent variables: force and distance. The results of ANOVA tests are shown in Table 4.

For separation forces, the P-values indicate that all factors are statistically significant, and the interactions between these factors are also statistically significant. It also finds, in terms of separation distances, all factors and their interactions are statistically significant too, except the interaction between all three factors which is not significant. The lack of interaction between all factors suggests that the joint effect of separation speed, film and resin is not as significant as the sum of effects for all factors. However, due to the large number of data collected in this experiment,

P-values are inclined to be small. Therefore, it is of interest to know the interactions between the factors too.

TABLE 4: 3-way ANOVA results

Force

Source	DF	Adj SS	Adj MS	F-Value	P-Value
Speed	1	660.6	660.65	1365.96	0.000
Film	1	589.7	589.66	1219.18	0.000
Matl	1	2848.6	2848.58	5889.71	0.000
Speed*Film	1	260.8	260.80	539.23	0.000
Speed*Matl	1	519.8	519.83	1074.79	0.000
Film*Matl	1	114.7	114.73	237.22	0.000
Speed*Film*Matl	1	307.4	307.40	635.58	0.000
Error	264	127.7	0.48		
Total	271	5429.3			

Distance

Source	DF	Adj SS	Adj MS	F-Value	P-Value
Speed	1	3.0644	3.0644	614.34	0.000
Film	1	16.7317	16.7317	3354.34	0.000
Matl	1	0.5860	0.5860	117.47	0.000
Speed*Film	1	0.9430	0.9430	189.05	0.000
Speed*Matl	1	0.1528	0.1528	30.64	0.000
Film*Matl	1	1.4433	1.4433	289.36	0.000
Speed*Film*Matl	1	0.0023	0.0023	0.46	0.499
Error	264	1.3169	0.0050		
Total	271	24.2403			

FIGURE 7 and 8 are main effects and interactions plots for separation forces and distances, respectively, which are all generated through Minitab. Main effects plots show differences between level means for all three factors, which each level connects through a line. if this line is horizontal, there is no main effect, vice versa. The slope of the line indicates the magnitude of effect, which steeper means greater. Interaction plots show the relationship between one factor and its response from another factor, in which one factor's level is on the x-axis and the other factor's levels are represented as individual lines. When those lines are parallel that means no interaction. However, when they are non-parallel lines, the greater the difference of slopes the stronger the interactions.

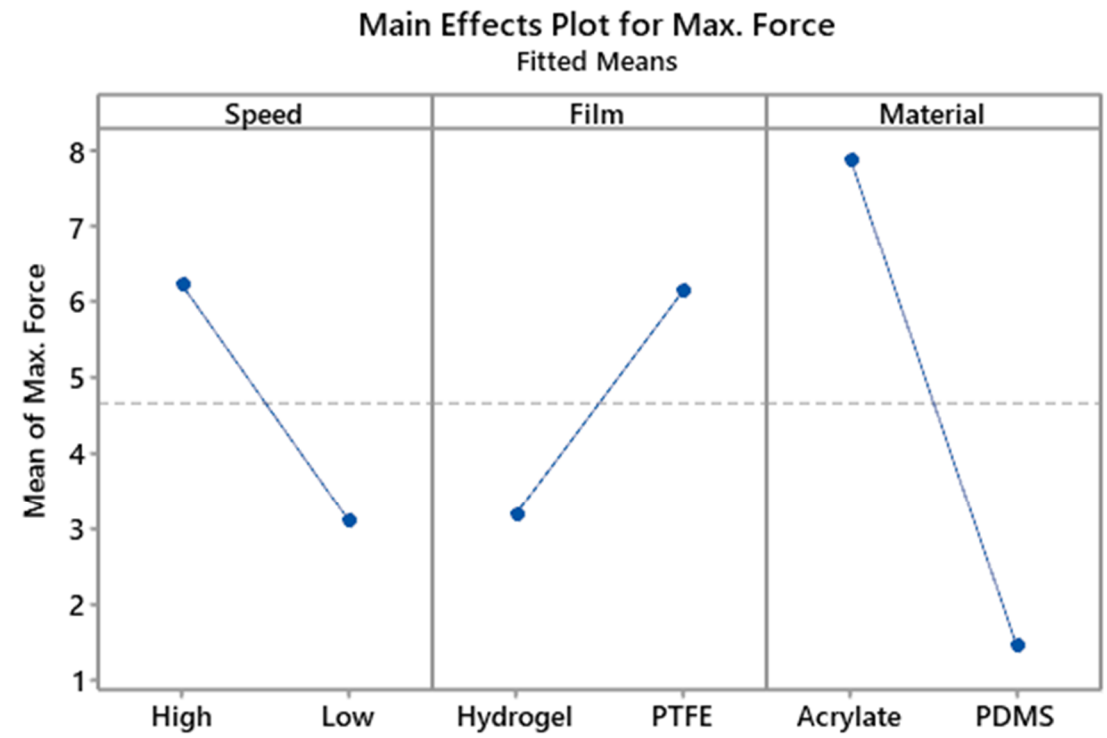

(a)

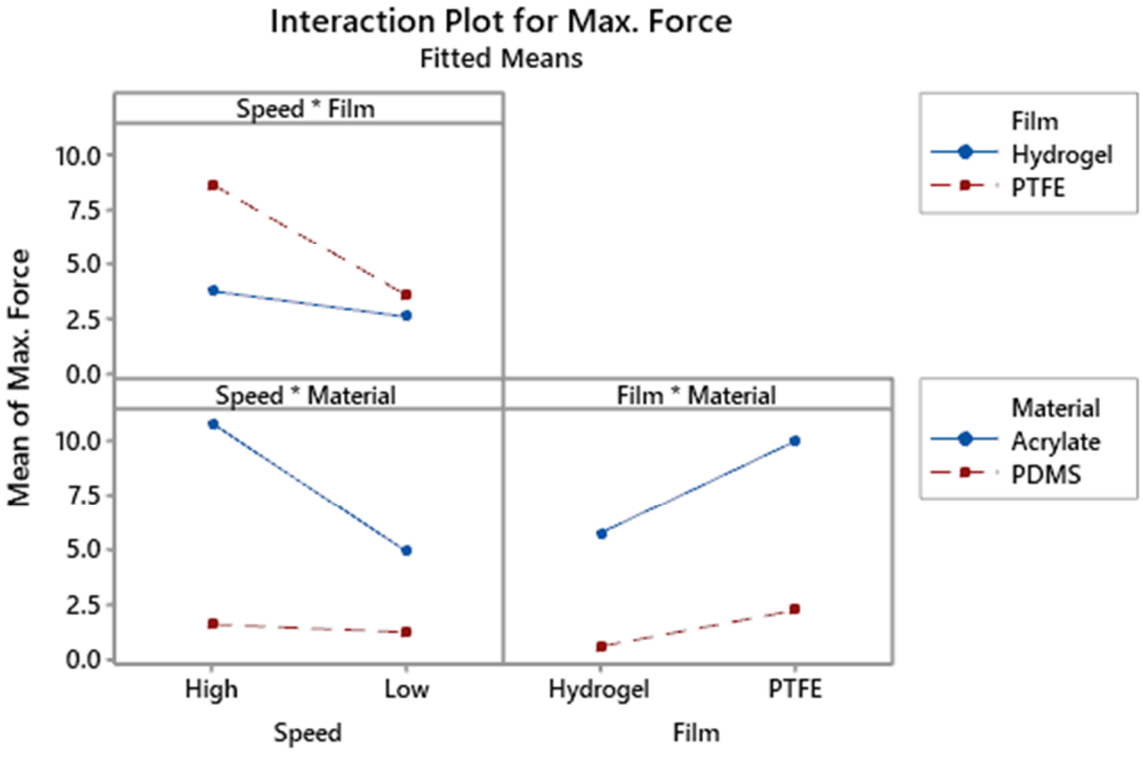

(b)

FIGURE 7: Three-way ANOVA on the separation force (a) Main effects; (b) Interactions

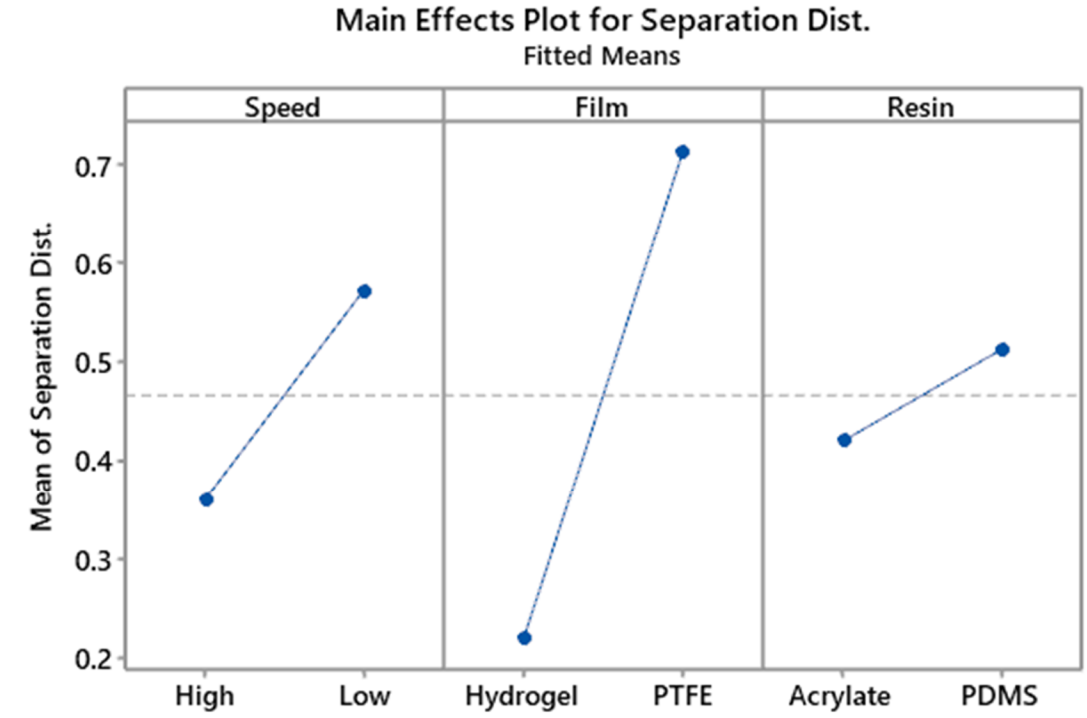

(a)

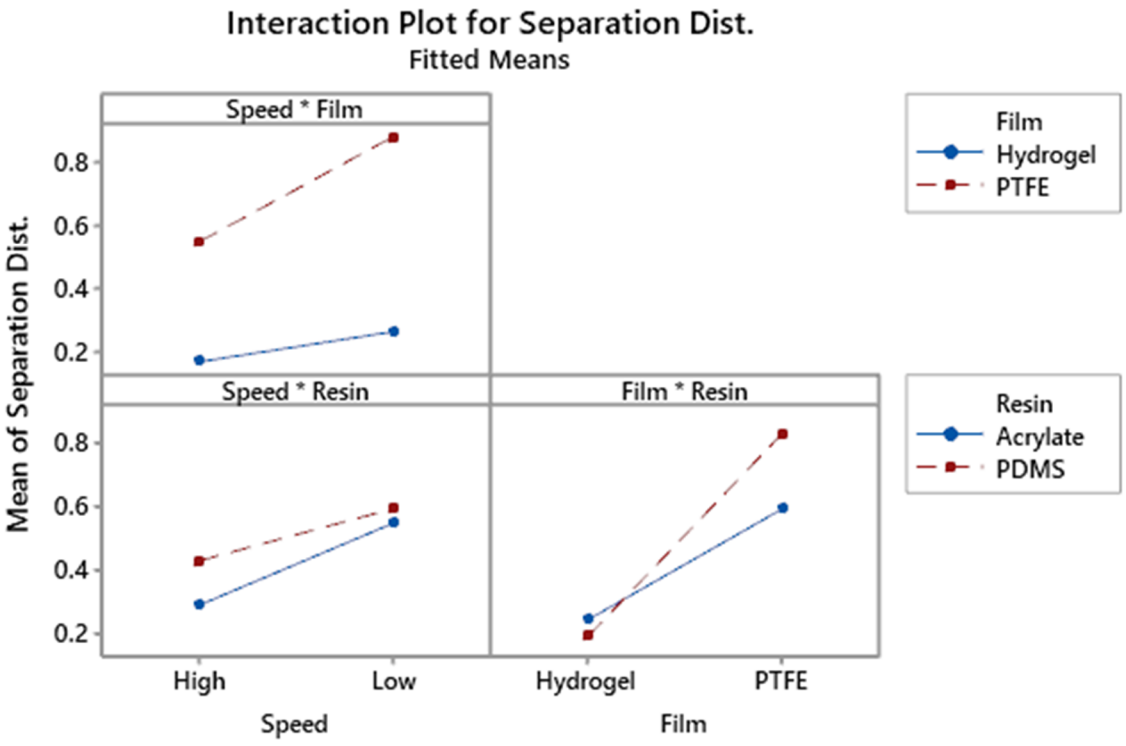

(b)

FIGURE 8: Three-way ANOVA on the separation distance (a) Main effects; (b) Interactions

FIGURE 7a shows the main effects plot for separation force. On average, the high-speed results in higher separation force than lower one, hydrogel shows a lower separation force in the two films used, and acrylate-based resin exhibits a higher separation force than PDMS resin. Furthermore, the resin materials seem to be the dominant factor out of the three in terms of separation force. In FIGURE 7b, the interactions between each of the two factors are shown. The interactions are there but nothing dramatic. From the Speed-Film interaction plot, the speed has more influence on PTFE film than hydrogel film in terms of separation force. The speed-material interaction indicates acrylate-based resin's separation force is more sensitive to separation speed than PDMS resin. The film-material plot demonstrates acrylate-based resin is slightly more subject to different vat films than PDMS resin. Moreover, the overall trends of both films suggest that faster the ascending speed, higher the separation force, which match with the main effects plots. The trends for the two resins also imply the same tendency on their individual main effects plot.

FIGURE 8a shows the main effect plots for the pulling distance, low-speed shows a longer separation distance than fast one, PTFE film exhibits a higher separation distance than hydrogel film, and PDMS resin generally has a slightly longer separation distance then acrylate-based resin. As for interaction plots on separation distance, all three interactions also exhibit similar inclinations and tendencies to their corresponding main effects. The film-material interaction plot for separation distance shows interception between the two effects. This is likely caused by the PDMS resin with hydrogel film case, which is contrary to the other resin and film combinations.

4. DISCUSSION

As discussed in the results section, all three factors have effects towards separation behavior. Therefore, it is necessary to address them individually on their effects and identify the potential explanations on their correlations to other factors.

4.1 Effects of Ascending Speed on Separation

The experiments show ascending speed effects both separation force and distance. With high-speed, the separation shows a larger force but shorter distance, and vice versa. This relationship between separation speed and separation force is consistent with findings in prior studies [6,20,21]. As separation speed goes up, the resultant stress in the cured part increases, which implies that force exerted on the same cross-sectional area also rises [21]. However, the correlation between speed and force may vary depending on the resin and film used, because of different tensile strength and shearing strength that each material has [21]. Evidence by the profile change in FIGURE 5 and 6, and interaction plot in FIGURE 7b, acrylate-based resin and PTFE film are more sensitive to separation speed than their counterparts. This difference may be related to their material's viscoelastic behavior, which causes the material, both part and film, to deform during the separation [20,21]. Because it varies between materials used for resin and film, we may not always have the luxury to optimize the separation speed for both materials.

4.2 Effects of Vat Film on Separation

This study finds that the hydrogel film exhibited lower separation forces and shorter separation distances compared to the PTFE film regardless of the materials and separation speeds used. Yet, the magnitude of those reductions may have other contributors than just the film itself. In both PDMS resin with hydrogel film cases, the results show a negligible separation force and distance. This may be the result of PDMS's low surface energy [22,23] and capability for oxygen

inhibition [6,24]. As the building platform along with the printed PDMS moves from resin slurry to open air above the vat and then back in the resin slurry through the entire printing process, there may be oxygen molecules that traps in the structure of printed PDMS, which may reduce separation force like the oxygen inhibition layer, as discussed in the introduction section, Although the two resin materials with different chemical compositions and properties are tested, the results depend on the resin's non-polar characteristic, which repelling from hydrogel film relies on. Despite the fact that results show a successful force and distance reduction, this is uncertain if hydrogel film will be as effective as in this experiment with other low-polarity resins, such as epoxy acrylate-based resins [25,26].

4.3 Effects of Resin on Separation

From this experiment, the photocurable PDMS resin demonstrates extremely low separation force compared to acrylate-based resin, yet at the same time, exhibits a slightly longer separation distance. As mentioned in the previous section, solid PDMS has low surface energy, which can reduce the separation force. On the other hand, cured PDMS also has a low modulus, which deforms during the separation and prolongs the actual separation [6,27]. To the contrary, acrylate-based resin has a relatively poor elasticity, as a result, minimal deformation occurs on the part, which may reduce separation distance [11]. Moreover, the in house PDMS resin is not optimized for not only the two relatively high separation speeds used in this experiment but also its low modulus and strength which may cause damage during the separation. This would affect the separation behaviors with PDMS resin [28].

Furthermore, the photoinitiator, TPO-L, used in this PDMS may affect the dimensional accuracy and printability because its characteristic peak is at 370 nm in ultraviolet-visible absorption spectrum, which is not the 403 nm that the DLP printer provides [10]. In a prior study on the effect of light wavelength on curable photopolymer resins, the depth of curing could vary

largely depending on the wavelength [30]. This variation may affect the quality of printed parts. This prolongs the exposure time to cure the PDMS resin, that is 7 times longer than its counterpart in this experiment, the commercial acrylate-based resin, may lead to over-curing or under-curing depending on the situation. For the same reason, the overall printing time is also not directly compared.

5. CONCLUSION

Through this study, the separation behavior of a constrained surface VP process with a photocurable PDMS resin is investigated systematically and quantitatively in terms of the influences on PTFE film and hydrogel film in comparison with a commercial acrylate-based resin. A DLP printer is modified with an in-situ force measuring capability. 8 test cases with unique film, resin, and separation speed are developed. The force profiles for each case are plotted and analyzed. It is found that all three factors influence the separation. Furthermore, the full-factorial experiments also proofed this conclusion. The following are the key findings of this study:

- Photocurable PDMS shows a lower separation force, but due to its low modulus it deforms and requires longer distances to fully separate.
- The hydrogel film demonstrates low separation force and distance with its repelling effect to non-polar resins.
- PDMS printing on hydrogel illustrates a small separation force, which may allow faster separation speed.

Through the experiments, there are also few limitations that need to be addressed. The resin materials used in this experiment are not optimized at the same level, where the commercial acrylate-based resin is made for the current setup and in-house PDMS resin is less optimal. This limits the experimental setup, including the ascending speed and the cross-sectional area of the printed geometry. Moreover, the film quality may also be factor here, since the manufacturing processes led to a possible variations between different films made at different batches. Based on those limitations in this study, the key learning points are below:

- Ascending speed during the separation is capped by the material properties of the resin. In this particular experiment, PDMS resin's low modulus is the key factor that limits the separation speed.
- Film quality is also a potential contributor to the separation behavior, thus controlling the thickness of each hydrogel film is important.
- The printed part's quality is not a key consideration in this experiment because of the lack of optimization on PDMS resin with the current setup.

This leads to some future investigation on the optimization of photocurable PDMS resin, which needs to improve its printability at high separation speed.

REFERENCES

1. Al Rashid, A., et al., Vat photopolymerization of polymers and polymer composites: Processes and applications. Additive Manufacturing, 2021. 47: p. 102279.

2. Westbeek, S., et al., Prediction of the deformed geometry of vat photo-polymerized components using a multi-physical modeling framework. Additive Manufacturing, 2021. 40: p. 101922.

3. Zhou, C., et al., Digital material fabrication using mas‹ imag… projection based stereolithography. Rapid Prototyping Journal, 2013. 19: p. 153-165.

4. Pagac, M., et al., A Review of Vat Photopolymerization Technology: Materials, Applications, Challenges, and Future Trends of 3D Printing. Polymers, 2021. 13(4).

5. Melchels, F.P.W., J. Feijen, and D.W. Grijpma, A review on stereolithography and its applications in biomedical engineering. Biomaterials, 2010. 31(24): p. 6121-6130.

6. Pan, Y., et al., Study of separation force in constrained surface projection stereolithography. Rapid Prototyping Journal, 2017. 23: p. 353-361.

7. Alamdari, A., et al., Effects of Surface Energy Reducing Agents on Adhesion Force in Liquid Bridge Microstereolithography. Additive Manufacturing, 2020. 36: p. 101522.

8. Lian, Q., et al., Oxygen-controlled bottom-up mask-projection stereolithography for ceramic 3D printing. Ceramics International, 2017. 43: p. 14956-14961.

9. Schmidleithner, C. and D. M. Kalaskar, Stereolithography. 3D Printing. 2018: IntechOpen.

10. Jin, J., et al., A vibration-assisted method to reduce separation force for stereolithography. Journal of Manufacturing Processes, 2018. 34: p. 793-801.

11. Kim, D.S., et al., Mechanical isotropy and postcure shrinkage of polydimethylsiloxane printed with digital light processing. Rapid Prototyping Journal, 2020. 26(8): p. 1447-1452.

12. Zheng, R., et al., 3D Printing of a Polydimethylsiloxane/Polytetrafluoroethylene Composite Elastomer and its Application in a Triboelectric Nanogenerator. ACS Applied Materials & Interfaces, 2020. 12(51): p. 57441-57449.

13. Hinton, T.J., et al., 3D Printing PDMS Elastomer in a Hydrophilic Support Bath via Freeform Reversible Embedding. ACS Biomaterials Science & Engineering, 2016. 2(10): p. 1781-1786.

14. Chen, Q., et al., 3D Printed Multifunctional, Hyperelastic Silicone Rubber Foam. Advanced Functional Materials, 2019. 29(23): p. 1900469.

15. Vondracek, P. and M. Schätz, Bound rubber and crepe hardenin‡ in silicone rubber. Journal of Applied Polymer Science, 1977. 21: p. 3211-3222.

16. Material Safety Data Sheet – SUPERFINE UV RESIN_CLEAR 500G×2, X. inc., Editor. 2017.

17. Kim, D.S., et al., Feasibility study of silicone stereolithography with an optically created dead zone. Additive Manufacturing, 2019. 29: p. 100793.

18. FlexiForceTM standard Model A101, T. inc., Editor. 2021.

19. CHANG, Y.-C. and T.-H. KUO, Stereolithography Elastic Film With Adjustable Peeling Force, in U.S. Patent Application Publication. 2019, XYZPRINTING , INC . , New Taipei City (TW) ; KINPO ELECTRONICS , INC . , New Taipei City (TW): United States.

20. Huang, Y.-M. and C.-P. Jiang, On-line force monitoring of platform ascending rapid prototyping system. Journal of Materials Processing Technology, 2005. 159(2): p. 257-264.

21. Ye, H., et al., Investigation of separation force for constrained-surface stereolithography process from mechanics perspective. Rapid Prototyping Journal, 2017. 23(4): p. 696-710.

22. He, H., et al., Effect of Constrained Surface Texturing on Separation Force in Projection Stereolithography. Journal of Manufacturing Science and Engineering, 2018. 140(9).

23. Kim, Y.G., et al., Study on the surface energy characteristics of polydimethylsiloxane (PDMS) films modified by C4F8/O2/Ar plasma treatment. Applied Surface Science, 2019. 477: p. 198-203.

24. Kudo, H., et al., A flexible and wearable glucose sensor based on functional polymers with soft-MEMS techniques. Biosensors & bioelectronics, 2006. 22 4: p. 558-62.

25. Bajpai, M., V. Shukla, and A. Kumar, Film performance and UV curing of epoxy acrylate resins. Progress in Organic Coatings, 2002. 44(4): p. 271-278.

26. Francis, L.F. and C.C. Roberts, Chapter 6 - Dispersion and Solution Processes, in Materials Processing, L.F. Francis, Editor. 2016, Academic Press: Boston. p. 415-512.

27. McCaig, M.S. and D.R. Paul, Effect of film thickness on the changes in gas permeability of a glassy polyarylate due to physical agingPart I. Experimental observations. Polymer, 2000. 41(2): p. 629-637.

28. Ajaj-Alkordy, N.M. and M.H. Alsaadi, Elastic modulus and flexural strength comparisons of high-impact and traditional denture base acrylic resins. The Saudi Dental Journal, 2014. 26(1): p. 15-18.

29. Wu, J., et al., Rapid digital light 3D printing enabled by a soft and deformable hydrogel separation interface. Nature Communications, 2021. 12(1): p. 6070.

30. Bennett, J., Measuring UV curing parameters of commercial photopolymers used in additive manufacturing. Additive Manufacturing, 2017. 18: p. 203-212.

APPENDIX A

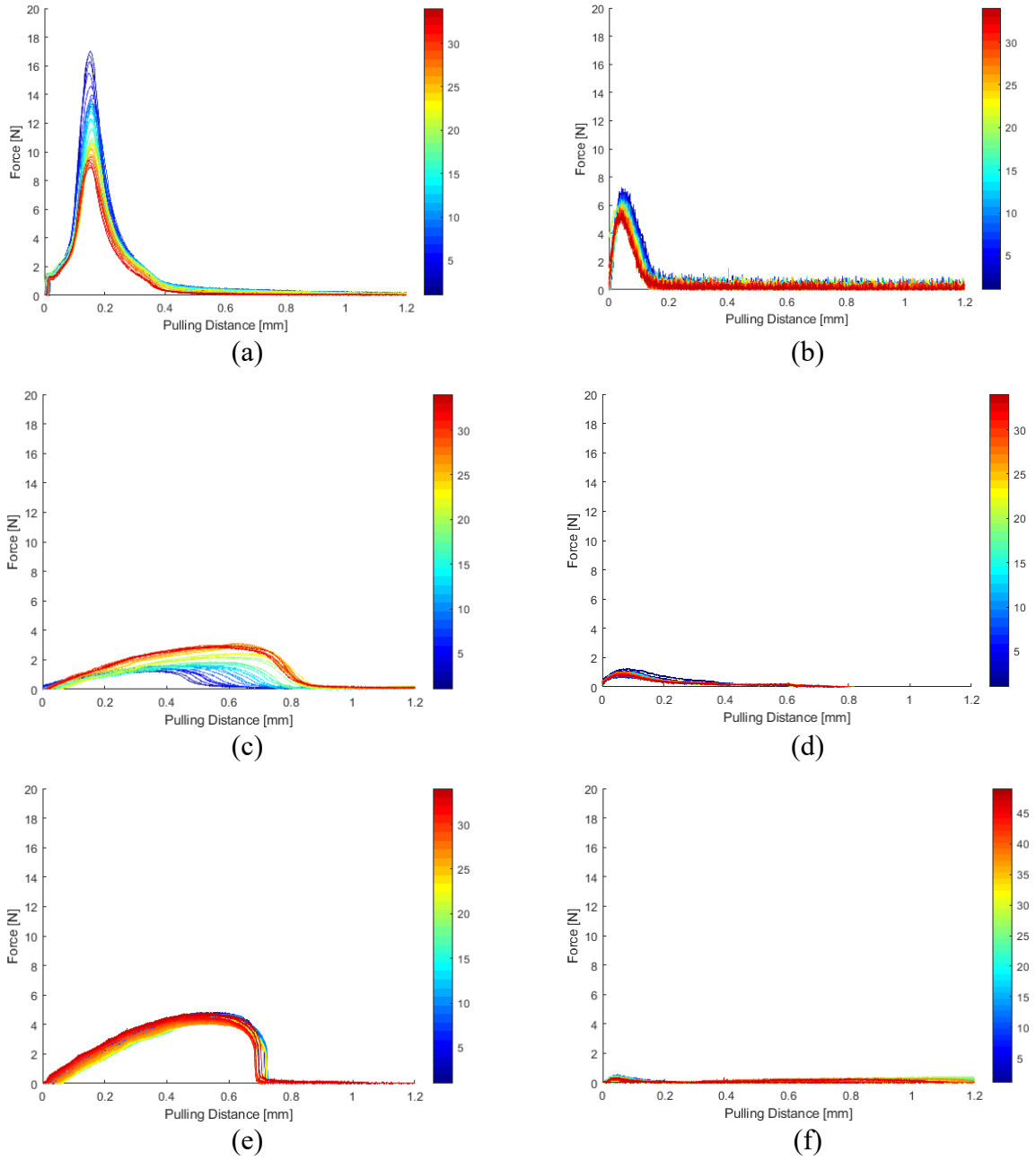

FIGURE A: Separation forces in the process of printing a 2.5 mm tall square extrusion – repeated cases a) case 1 b) case 2 c) case 3 d) case 4 e) case 5 f) case 8